Preprint of paper presented at the 12th European Wave and Tidal Energy Conference, Cork, Ireland, August 2017

Efficient Modelling of Seabed Friction and Multi-Floater Mooring Systems in MoorDyn

Matthew Hall
School of Sustainable Design Engineering, University of Prince Edward Island, Canada
E-mail: mthall@upei.ca

***Abstract*—This paper discusses two important additions under development in MoorDyn, a computationally-efficient lumped-mass model for simulating the dynamics of mooring systems. The first is a means of modelling friction between mooring lines and the seabed. A simple saturated-damping approach is demonstrated, and tests with steady lateral motion show reasonable behaviour from this initial implementation. The second capability under development is modelling mooring systems attached to more than one floating body. This is relevant for new design ideas that see moorings attached to multi-body structures or shared among an entire array of floating energy devices. A means of coupling about a collection of independently-moving fairlead connections has been implemented. The resulting capability is demonstrated with a scenario involving a mooring line connecting two bodies undergoing circular motions. Seabed friction is also included in the scenario, showing the effect that such friction can have in altering the mechanical power dissipated by the moorings in a shared-mooring wave energy array. Lastly, some ideas are presented for wave tank tests that could be used to validate these newly-implemented model components.**

***Keywords*—mooring, dynamics, modelling, seabed friction, multi-floater.**

I. Introduction

This paper discusses the representation of friction in computationally-efficient mooring models and how such models can also support scenarios where moorings are shared between multiple floating bodies.

Friction between mooring lines and the seabed can have an important influence on the dynamics of catenary mooring systems. Even in laboratory tests with smooth concrete basin floors, friction is thought to noticeably affect the measured mooring tensions [1]. Modelling such friction is not new (e.g. [2]); however, the choice of appropriate approach depends on the level of fidelity of the overall modelling framework.

A second capability under development is modelling mooring systems attached to more than one floating body. This is relevant for new design ideas that see moorings shared among an entire array of floating energy devices (e.g. [3]–[6]). It is also applicable to single devices that have articulated or flexible bodies, such as is the case for many wave energy converter (WEC) designs. While in most cases the modelling of such scenarios does not require fundamental advances in methods, it does require strategic arrangement of a model's calculation process, particularly when versatility in coupling to other modelling tools is required.

The exploration of modelling seabed friction and multi-body mooring interconnections discussed in this paper is aimed at efficient and versatile modelling of mooring system dynamics. As such, higher levels of detail such as the bending behaviour of undersea cables are intentionally neglected. The focus here is mooring behaviour as it pertains to mooring system design and loads analysis.

The literature is rich with techniques for modelling the dynamics of mooring lines and undersea cables. These are reviewed in other works such as [7]–[9]. In recent years, a number of simpler but more mature and accessible mooring modelling implementations have emerged. MAP is a quasi-static mooring model that set the standard as an open-source mooring simulator versatile enough to be used in conjunction with many different modelling tools [10]. MoorDyn followed a similar distribution model, but used a lumped-mass formulation to provide modelling of mooring dynamics [11]. Two other codes, OPASS [12] and MooDy [13], are not open source but provide a somewhat more advanced formulation when it comes to mooring line elasticity.

The emergence of these various codes in the literature reflects the reality that many mooring modelling needs can be satisfied by relatively simple approaches. In many cases, the limiting factors in applied mooring modelling are not to do with the order of a model's finite elements but in the versatility of the model—whether it can be applied to different scenarios and whether it can integrate with other analysis tools. In that context, the work described in this paper is a step toward increasing the versatility of MoorDyn to better account for scenarios involving seabed friction and shared moorings. MoorDyn uses a simple spring-damper model for axial elasticity, and represents hydrodynamics forces using Morison's equation. Vertical seabed-contact forces are handled by a spring-damper approach activated whenever nodes pass below the defined seabed height.

With its simple formulation, MoorDyn has shown to be computationally efficient and also suitably accurate for common offshore renewable energy mooring scenarios [1], [11], [14], [15]. It was intended to capture only the most essential phenomena relevant to typical floating wind turbine mooring systems, accurately predicting overall line tensions while prioritizing computational efficiency. To achieve this efficiency, it is common to use only around 20 segments per mooring line. As additional capabilities are added to increase the range of situations that can be adequately modelled, these new capabilities need to be appropriate to the coarsely discretized model implementation. A particular challenge is that the coarse discretization can cause nonphysical tension transients from the step changes in contact forces that occur when nodes arrive or depart from the seabed.

The following sections present steps towards modelling seabed friction and multi-floater mooring arrangements in MoorDyn, before discussing possibilities for validation and finally the remaining model development steps to be completed.

II. Seabed Friction

The seabed friction models discussed in the literature range from simple one-equation approaches for resisting sliding to complex multi-component approaches that account for rapid impacts as well as sliding and static friction. Liu and Bergdahl [16] describe a time-domain approach in which the dynamic friction force is represented by a linear damping behaviour that is saturated at a minimal velocity to a value equal to the friction coefficient multiplied by the normal contact force. The damping representation allows for stable behaviour when sliding velocities are near zero.

An adjusted approach is given by Azcona et al [12], whereby a stiffness-based model is used to represent the static friction behaviour when sliding motion is negligible, providing a more true sticking behaviour than a damping-based approach. When the static friction is overcome, the friction force saturates similarly to the damping approach to provide a dynamic friction behaviour.

Wang et al. [17] describe a more involved seabed interaction model that includes additional terms to govern the transition of the friction behaviour between sticking and sliding states. Their model also includes terms for impact and rebound behaviour as well as the loss of momentum incurred in such cases due to seabed friction during the impact.

A. Seabed Contact Implementation

Seabed contact in MoorDyn is only considered when a node's z coordinate, r_3, is less than or equal to that defined for the seabed, z_b. The vertical seabed contact force is modelled as

$$B_3 = [(z_b - r_3)k_b - \dot{r}_3 c_b]\, d\, l \tag{1}$$

where k_b and c_b are stiffness and damping coefficients for the seabed, respectively, d is line diameter, and l is line segment length.

The seabed friction approach being implemented in MoorDyn is that of [16], since this damping model is easy to realize and less likely to suffer from artifacts caused by a coarse discretization. If μ is the friction coefficient between the mooring line and the seabed, $\dot{r}_1$ and $\dot{r}_2$ are sliding velocities in x and y, and B_3 is the normal contact force, then the friction force magnitude is calculated as

$$F_f = \min\left(C_f\sqrt{\dot{r}_1^2 + \dot{r}_2^2},\ 1\right)\mu\, B_3 \tag{2}$$

where C_f is a damping coefficient chosen to be as large as possible without inducing alternating friction forces at each time step. The friction forces acts in opposition to the direction

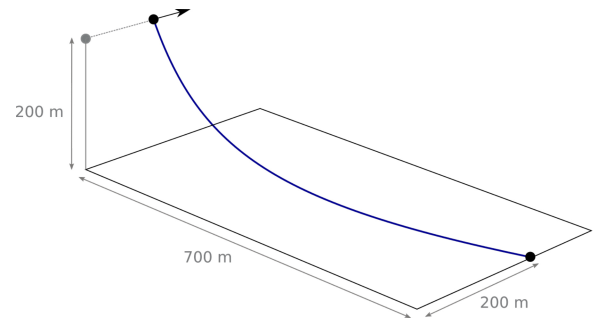

Fig. 1. Seabed friction scenario with fairlead motion in y direction.

of movement, so the component friction forces in x and y can be expressed as

$$B_1 = -\min\left(C_f\sqrt{\dot{r}_1^2 + \dot{r}_2^2},\ 1\right)\mu B_3 \frac{\dot{r}_1}{\sqrt{\dot{r}_1^2 + \dot{r}_2^2}} \tag{3}$$

$$B_2 = -\min\left(C_f\sqrt{\dot{r}_1^2 + \dot{r}_2^2},\ 1\right)\mu B_3 \frac{\dot{r}_2}{\sqrt{\dot{r}_1^2 + \dot{r}_2^2}}. \tag{4}$$

B. Seabed Friction Demonstration

To show the behaviour of the friction model, a single mooring line is subjected to a prescribed linear motion of the fairlead: moving at 0.8 m/s for 500 seconds. The mooring line is set up to represent that of a typical semisubmersible floating wind turbine, with properties similar to those used in previous work [11]. As illustrated in Fig. 1, the anchor is positioned 700 m in the x direction and 200 m in the y direction from the initial fairlead position, and the water depth is 200 m. At an unstretched length of 800 m, more than half the mooring line length is in contact with the seabed so the fairlead motion results in significant sliding seabed contact. Three friction coefficients are used: 0, 0.05, and 0.1.

The plots of Figure 2 show a birds eye view of the mooring line profile at different instants in time as it responds to the fairlead motion. Each subplot corresponds to a different friction coefficient. The lumped-mass node points along the line are clearly marked, and those nodes in contact with the seabed are indicated by black dots. The closer spacing of the nodes near the left side of the plots reflects that the mooring line has a greater slope in the vertical plane near the fairlead. Comparing the plots, the effect of seabed friction can be clearly seen in the more curved mooring line profile. Interestingly, this change also coincides with a different amount of seabed contact.

The sensitivity to discretization is apparent from comparing results with the mooring line divided into 10, 20, and 40 segments. The 0.1 friction coefficient is used for this. The profile of the mooring line as seen from above is compared in Figure 3. Very little difference, even at a discretization of 10 segments, is visible from this perspective. A closer examination of just the y position of the line midpoint is shown in Figure 4 and this reveals a difference of perhaps 1% between 10 and 20 segment discretizations, and a much smaller difference between 20 and 40 segment discretizations.

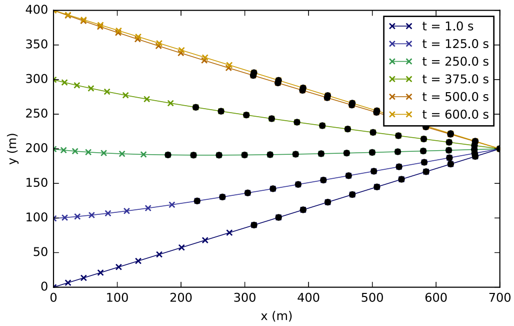

(a) $\mu = 0$

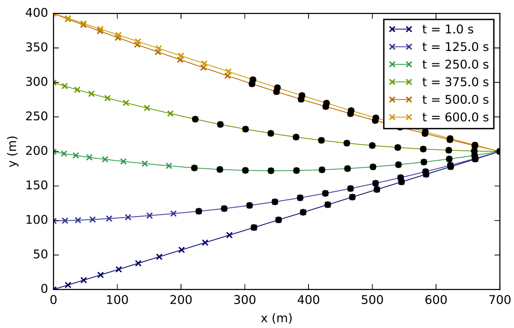

(b) $\mu = 0.05$

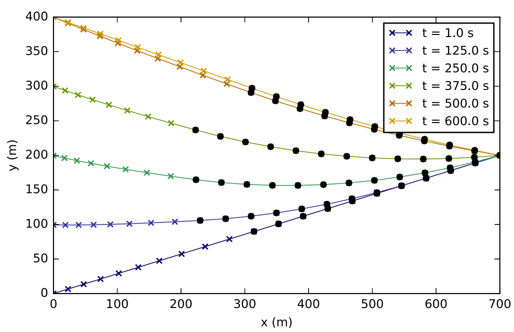

(c) $\mu = 0.1$

Fig. 2. Birds-eye view snapshots of mooring line profile during steady 0.8 m/s fairlead motion with three different friction coefficients. Nodes in contact with the seabed are dotted.

This affirms the adequacy of a 20 segment discretization for this type of analysis.

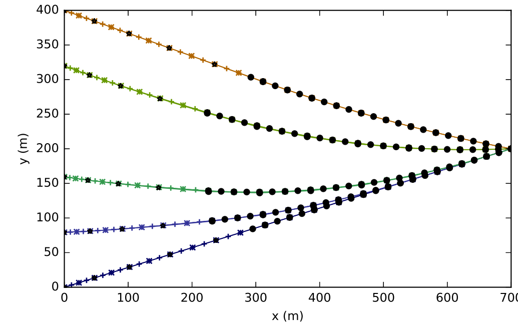

Fig. 3. Birds-eye view snapshots of mooring line profile during steady 0.8 m/s fairlead motion with $\mu = 0.1$ for three different discretization levels. Nodes in contact with the seabed are dotted.

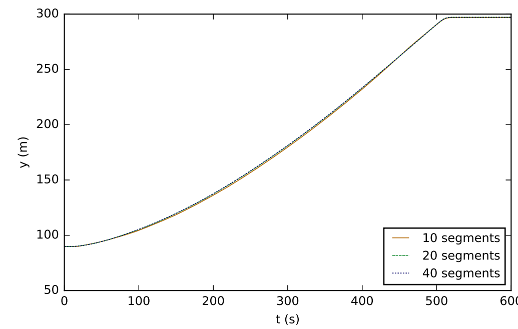

Fig. 4. y position of mooring line midpoint during steady fairlead motion scenario with $\mu = 0.1$ for three different discretization levels.

III. Multi-Floater Mooring Connections

One of the goals for MoorDyn is to be versatile in the types of scenarios that can be modelled. Previous work showed the capabilities in terms of interconnections between mooring lines and basic modelling of clump weights and floats [18]. This is of value for complex moorings of a single structure. The next step in generality is to allow modelling of multiple floating bodies. This is enabled by a new coupling function that accepts the kinematics of each fairlead point, and returns the resulting point reactions forces, at each time step. This increases the ways that MoorDyn can be used—allowing modelling of, for example, an array of WECs with a shared mooring system, or multi-body WECs with moorings attached at various points. The time integration is handled the same way with this approach as with the rigid-body coupling approach: via a second-order Runge Kutta scheme.

A. Two-Floater Demonstration

A scenario with two floating bodes connected by one mooring line provides a simple demonstration of the multi-floater coupling ability. To begin with, the motions of the floating bodies are prescribed rather than using a full two-way coupling. This provides more controlled conditions and allows for precise adjustment of relative motion between the two floats. For this scenario, illustrated in Figure 5, the floats are taken to move in circular orbits of 5 m radius and 20 s period. The phase relationship between left and right floats is given by angle ϕ. A mooring line with the same material properties as used previously connects the two bodies at a distance of 100 m. The motions are centered at a depth of 10 m and the unstretched mooring line length is 150 m.

Snapshots of the vertical line profile are shown in Figure 6. The three subplots correspond to different phase relationships between the two bodies' motions. These plots demonstrate the modelling of multiple independently-moving connection points.

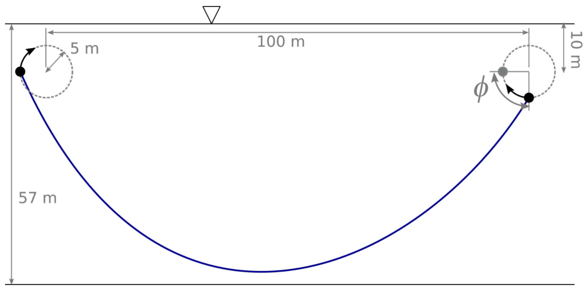

Fig. 5. Simulated scenario of a mooring line connecting two points moving in circular paths with phase difference, ϕ.

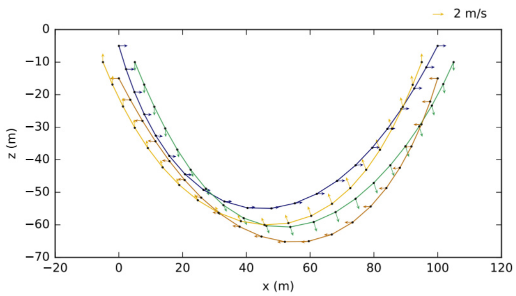

(a) 0 degree phase difference

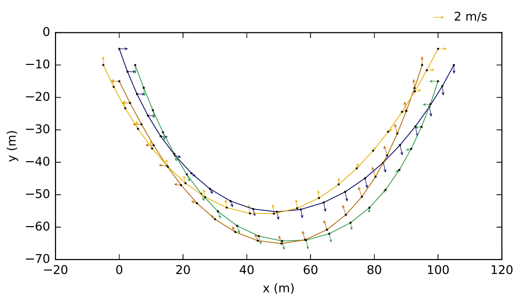

(b) 90 degree phase difference

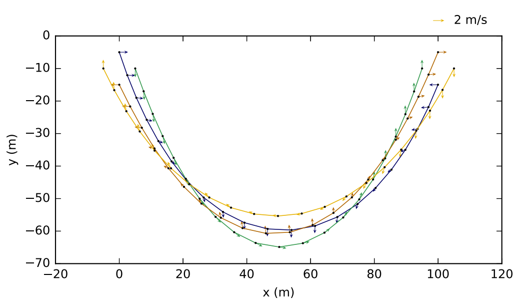

(c) 180 degree phase difference

Fig. 6. Vertical x-z plane snapshots of mooring line profile between two bodies undergoing orbital motion at three different phase relationships. Arrows indicate node velocities.

The seabed interaction discussed earlier can be added to the simulation by imposing a seabed depth that overlaps with the line profiles shown in Figure 6. A depth of 57 m makes it so that seabed contact is intermittent over the period of motion.

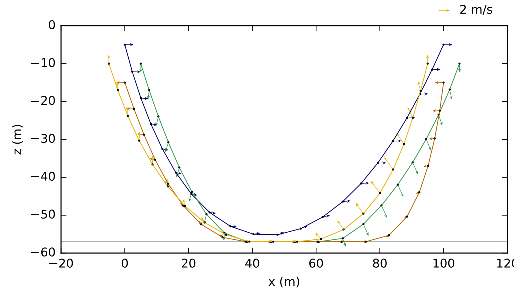

(a) 0 degree phase difference

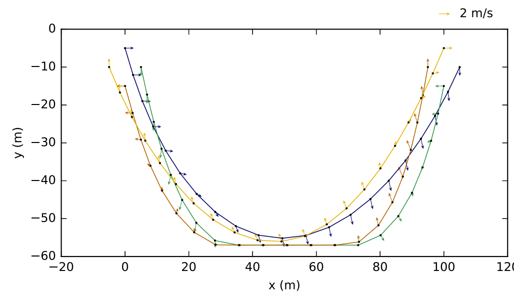

(b) 90 degree phase difference

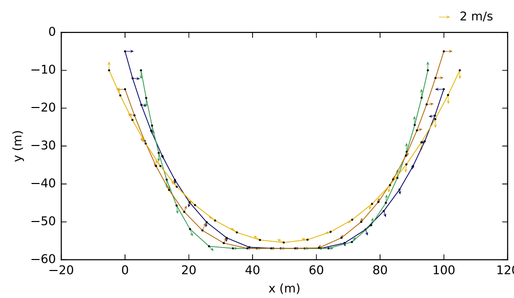

(c) 180 degree phase difference

Fig. 7. Vertical x-z plane snapshots of mooring line profile between two bodies undergoing orbital motion at three different phase relationships when seabed contact is included. Arrows indicate node velocities.

The resulting line profiles are shown in Figure 7. A friction coefficient of 0.1 was used for these simulations. Comparing Figure 6c with Figure 7c, the effect of the friction in resisting motion across the seabed and thereby making the profiles less symmetrical can be clearly seen.

Figure 8 shows the periodic tensions at each end of the mooring line for the three different phase offsets. Transients are visible in each signal. These arise when nodes touch down on the seabed—a clear artifact caused by the coarse discretization. The impulses caused by these node impacts are seen to decay after 5-10 cycles due to damping in the model. This emphasizes that seabed interaction is the area of model performance most affected by using a coarse discretization.

The mechanical power transfer from float to mooring line varies periodically with the motion. This is plotted in Figure 9. An interesting aspect of mooring drag and friction is how they add damping to the floats. This can be looked at in terms of

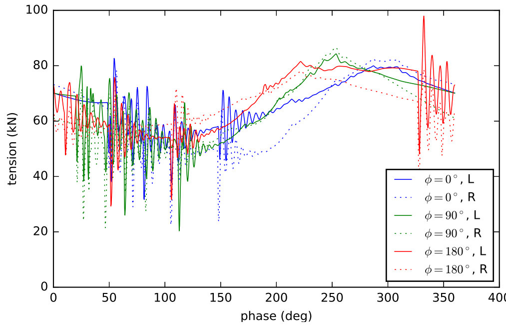

Fig. 8. Tension at fairlead connection over one period of motion.

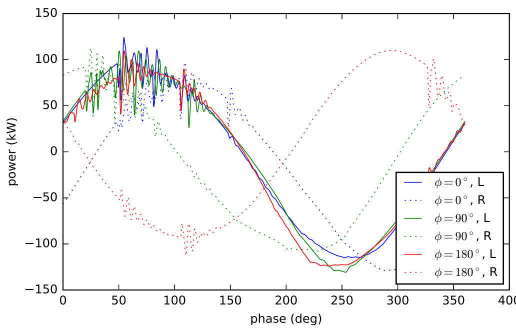

Fig. 9. Mechanical power exerted by float through fairlead connection over one period of motion.

the mechanical power transmitted or absorbed by the float via the mooring line fairlead as a consequence of the periodic motion. Table 1 shows the average mechanical power exerted in the tests previously discussed as well as how they change when friction is disabled.

TABLE I
MEAN POWER EXERTED BY FLOAT ONTO MOORING LINE

phase offset (deg)	0		90		180	
float (left/right)	L	R	L	R	L	R
friction (kW)	7.3	13.5	10.8	21.9	8.4	-1.7
no friction (kW)	6.5	21.6	7.9	14.8	10.5	-3.1

It is worth noting that the change in mean mechanical power taken from (or imparted to) each float by the presence of mooring friction is significant. Furthermore, these differences are with a friction coefficient of 0.1, whereas design standards such as DNV-OS-E301 recommend a friction coefficient of 1.0 for chain moorings on typical seabeds [19]. Clearly, seabed friction can be of relevance to wave energy converter behaviour in cases where there is significant seabed contact of the moorings.

IV. Towards Validation

The simulated scenarios discussed in this work, which are relatively simple, are relevant not just as demonstrations of the capabilities being developed but also as potential test scenarios for use in validation of these capabilities.

Constant-speed fairlead tow tests, as simulated in Section II, provide an easily-implemented way to reveal seabed friction in controlled conditions. Optical tracking, such as used by Azcona et al. [12], can be used to produce data that matches the plots of Figure 2. Validation of friction models then follows easily.

For modelling of multiple floating bodes interconnected by moorings, the question is not so much about the mooring or float modelling (since either of these models can be validated in isolation) but rather about the coupling of these models and whether the included assumptions hold true in the multi-body case. These questions can be tested in a relatively controlled manner by scenarios such as those simulated in Section III. By testing simple floating bodies interconnected by a mooring line and spaced at the correct distance, there are few additional phenomena at play that would detract from the main focus: how the interconnected floats interact. The approach of using regular waves, and adjusting the wavelength or float spacing to achieve various wave excitation phase differences between the two floats, makes for a simple and easily processed scenario for validation.

V. Conclusions and Future Work

The work presented here included a first attempt at seabed friction modelling. Ongoing work will seek to refine this initial attempt to account for more phenomena related to seabed interaction and friction, such as stick-slip behaviour, directional friction coefficients, and inclined seabeds. Also presented was the new coupling capability that allows a mooring system to be connected to multiple independent coupling points. A simple example demonstrates the type of scenario that can be realized as well as how the interaction with seabed friction can constitute a damping effect on arrays of floating devices that depends heavily on the phase relationships between device motion.

Non-physical tension transients were identified during node touchdown events as a result of the seabed contact model when the discretization is relatively coarse. An important direction of future work is to seek ways to reduce these transients without increasing the number of nodes.

Lastly, validation will be an important part of supporting the new features that are being developed. A new wave tank is currently under construction at the University of Prince Edward Island to facilitate suitable validation experiments.

References

[1] F. F. Wendt, M. T. Andersen, A. N. Robertson, and J. M. Jonkman, "Verification and validation of the new dynamic mooring modules available in FAST v8," in *Proceedings of the Twenty-sixth International Offshore and Polar Engineering Conference*, Rhodes, Greece, Jun. 2016.

[2] J. Azcona, T. A. Nygaard, X. Munduate, and D. Merino, "Development of a code for dynamic simulation of mooring lines in contact with seabed," in *EWEA Offshore 2011*, Amsterdam, The Netherlands, 2011.

[3] C. M. Fontana, S. R. Arwade, D. J. DeGroot, A. T. Myers, M. Landon, and C. Aubeny, "Efficient multiline anchor systems for floating offshore wind turbines," in *Proceedings of the 35th International Conference on Ocean, Offshore and Arctic Engineering*, Busan, South Korea, Jun. 2016.

[4] Z. Gao and T. Moan, "Mooring system analysis of multiple wave energy converters in a farm configuration," in *Proceedings of the 8th European Wave and Tidal Energy Conference*, Uppsala, Sweden, 2009.

[5] M. Goldschmidt and M. Muskulus, "Coupled mooring systems for floating wind farms," *Energy Procedia*, vol. 80, pp. 255–262, Jan. 2015.
[6] P. Connolly, K. Devries, and M. Hall, "Shared mooring systems for floating offshore wind farms," in *Offshore Energy and Storage Symposium*, Cape Cod, USA, Jun. 2017.
[7] M. Masciola, J. Jonkman, and A. Robertson, "Extending the capabilities of the mooring analysis program: A survey of dynamic mooring line theories for integration into FAST," in *Proceedings of the 33rd International Conference on Ocean, Offshore and Arctic Engineering*, San Francisco, California, USA, Jun. 2014.
[8] M. Hall, B. Buckham, and C. Crawford, "Evaluating the importance of mooring line model fidelity in floating offshore wind turbine simulations," *Wind Energy*, vol. 17, no. 12, pp. 1835–1853, Dec. 2014.
[9] B. S. Kallesoe and A. M. Hansen, "Dynamic mooring line modeling in Hydro-Aero-Servo-Elastic wind turbine simulations," in *Proceedings of the Twenty-first International Offshore and Polar Engineering Conference*, Maui, Hawaii, USA, Jun. 2011.
[10] M. Masciola, J. Jonkman, and A. Robertson, "Implementation of a multisigmented, Quasi-Static cable model," in *Proceedings of the Twenty-third (2013) International Offshore and Polar Engineering Conference*, Anchorage, Alaska, USA, Jul. 2013.
[11] M. Hall and A. Goupee, "Validation of a lumped-mass mooring line model with DeepCwind semisubmersible model test data," *Ocean Engineering*, vol. 104, pp. 590–603, 2015.
[12] J. Azcona, X. Munduate, L. González, and T. A. Nygaard, "Experimental validation of a dynamic mooring lines code with tension and motion measurements of a submerged chain," *Ocean Engineering*, vol. 129, pp. 415–427, Jan. 2017.
[13] J. Palm, G. Moura Paredes, C. Eskilsson, F. Taveira Pinto, and L. Bergdahl, "Simulation of mooring cable dynamics using a discontinuous galerkin method," in *Proceedings of V International Conference on Computational Methods in Marine Engineering*, Hamburg, Germany, May 2013.
[14] S. Sirnivas, Y. Yu, M. Hall, and B. Bosma, "Coupled mooring analysis for the WEC-Sim wave energy converter design tool," in *Proceedings of the 35th International Conference on Ocean, Offshore and Arctic Engineering*, Busan, South Korea, Jun. 2016.
[15] M. T. Andersen, F. T. Wendt, A. N. Robertson, J. M. Jonkman, and M. Hall, "Verification and validation of multisegmented mooring capabilities in FAST v8," in *Proceedings of the Twenty-sixth International Offshore and Polar Engineering Conference*, Rhodes, Greece, 2016.
[16] Y. Liu and L. Bergdahl, "Influence of current and seabed friction on mooring cable response: comparison between time-domain and frequency-domain analysis," *Engineering Structures*, vol. 19, no. 11, pp. 945–953, Nov. 1997.
[17] F. Wang, G.-l. Huang, D.-h. Deng, and X.-h. Tu, "A study on dynamic response of cable-seabed interaction," *Journal of Shanghai Jiaotong University (Science)*, vol. 14, no. 4, pp. 443–449, Aug. 2009.
[18] G. Vissio, B. Passione, M. Hall, and M. Raffero, "Expanding ISWEC modelling with a Lumped-Mass mooring line model," in *Proceedings of the 11th European Wave and Tidal Energy Conference*, Nantes, France, Sep. 2015.
[19] DNV, "DNV-OS-E301: position moorings," Det Norske Veritas, Hovik, Norway, Tech. Rep., Oct. 2013.